Electronic Supplementary Material (ESI) for Lab on a Chip
This journal is © The Royal Society of Chemistry 2020

Supporting Information

An integrated biomimetic array chip for high-throughput co-culture of liver and tumor microtissues for advanced anticancer bioactivity screening

Yu Hou,‡[a] Xiaoni Ai,‡[a] Lin Zhao,[a] Zhao Gao,[a] Yujiang Wang,[a] Yingyuang Lu,[a] Pengfei Tu,[a] Yong Jiang*[a]

[a] State Key Laboratory of Natural and Biomimetic Drugs, School of Pharmaceutical Sciences, Peking University, Beijing 100191, China

‡ These authors contributed equally to this work.

* *Corresponding author.*

Yong Jiang

E-mail address: yongjiang@bjmu.edu.cn

Tel: +86 10 82802719

1. Supplementary methods

1.1 Drug sensitivity with various cell types to 5-FU

Four types of tumor cells were used as candidates for construction of the 3D tumor microtissues, including DU145 cells, U251 cells, HCT116 cells and MCF7 cells. Approximately 3000 tumor cells with various types were seeded into 384-well plates and incubated overnight. Next, EMEM medium containing 10 μM 5-FU was added for 48 h treatment. The CCK-8 working solution was added to each well for detection of cell viability at 450 nm by a microplate reader.

1.2 Establishment of standard curves for quantification of CES activities

Activity of CES enzyme was quantified using standard curves. The residual p-nitrophenylacetate (PNPA) concentration was determined based on a standard curve prepared in PBS with 0, 4.7, 9.4, 18.8, 37.5, 75, 150 and 300 μM PNPA.

1.3 Cell viability and functionality assessment of primary human hepatocytes (PHHs)

PHHs were mixed with a rat tail type I collagen at a ratio of 2:1 on ice. The mixture was pipetted in the microwell to obtain 5000 cells per well. The final concentration of the type I collagen in the cell-collagen mixture was 1.67 mg/mL. The liver chip was incubated at 37 °C for 20 min for gelation before InVitroGro CP medium supported with 10% fetal bovine serum was introduced into the reservoirs. The 3D PHH was then placed in a humidified chamber with 5% CO_2 at 37 °C. The culture medium was changed every 24 h. Viability of the PHH in the liver chip was detected at 3, 5, 7, 10, and 15 days using CellTiter blue working solution. Cell viability was determined by

dividing fluorescence intensity of each microwell with the seeded cell number. Concentrations of the albumin and urea production were detected at 15-day culture by a human albumin ELISA kit (Bethyl laboratories, USA) and a colorimetric urea assay kit (abcam, USA) according to the manufacturer's instruction, respectively. The productions of albumin and urea were expressed as μg albumin per day and per million PHH (μg/million cells/day) and μmol urea per day and per million PHH (μmol/million cells/day).

2. Supplementary figures

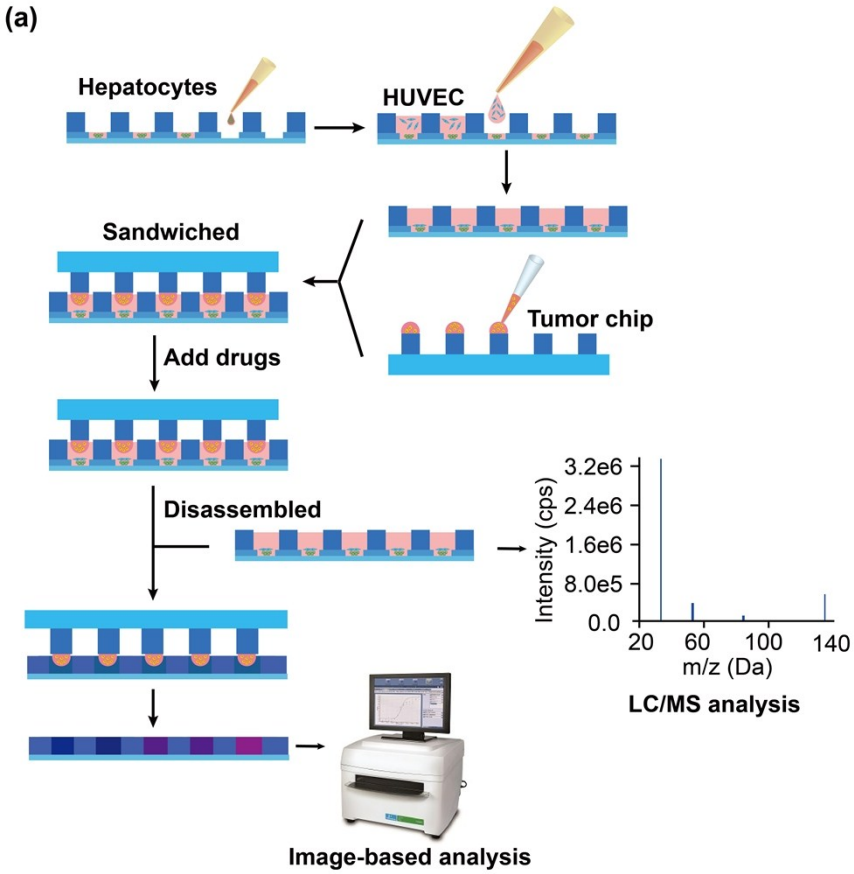

Fig. S1. Operation of the iBAC for benchtop assays.

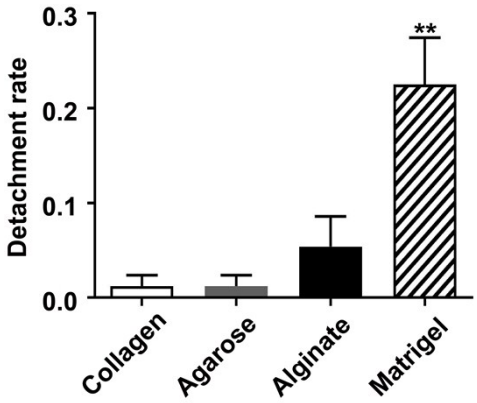

Fig. S2. Comparison of different biomaterials on cross-shaped protrusions for immobilization of 3D tumor microtissues. $n = 48$. All data are presented as means ± SD from three independent experiments. $^{**}p < 0.01$, relative to control group.

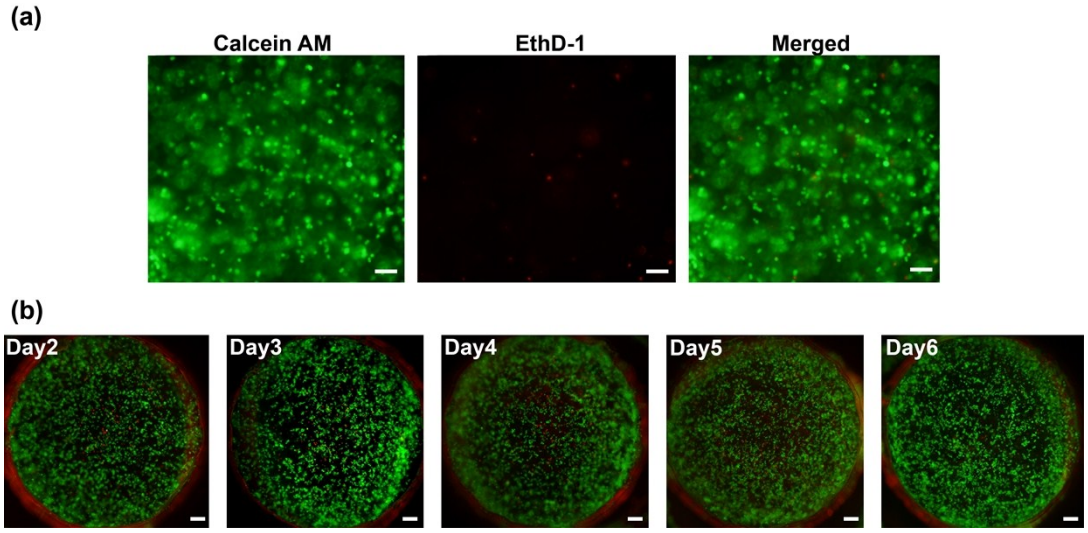

Fig. S3. Viability assessment. (a) Viability of 3D tumor microtissue on the tumor chip. Scale bar: 100 μm. (b) Viability of 3D biomimetic liver microtissue on the liver chip. There were no detrimental effects on the cells survival for 6 days on the iBAC. Scale bar: 200 μm. Live cells were stained with green and dead cells were stained with red.

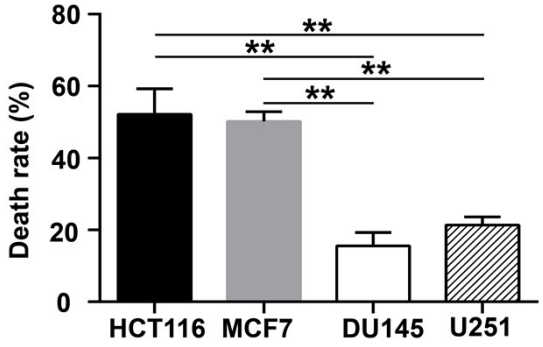

Fig. S4. Drug sensitivity of different cell types to 5-FU. All data are presented as means ± SD from three independent experiments. $^{**}p < 0.01$, *t*-test between groups.

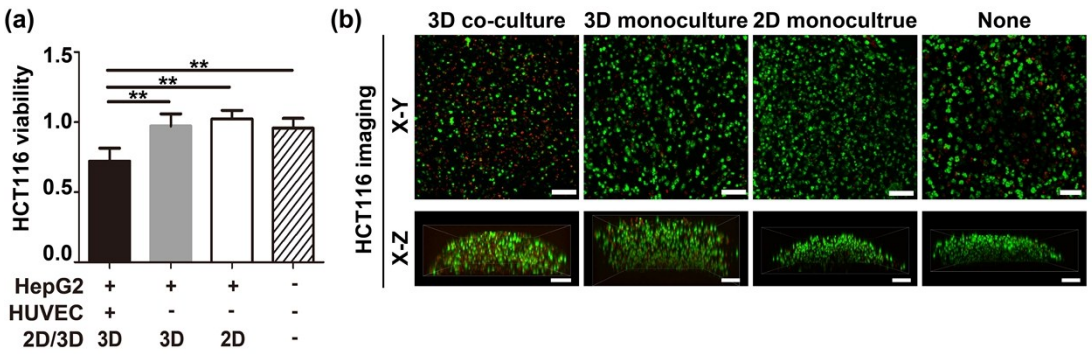

Fig. S5. Viabilities of 3D HCT116 cells co-cultured with different liver models were compared by CellTiter Blue (a) and confocal microscopy (b). The three liver models were 3D biomimetic liver microtissue (3D-Hep-HUVEC), 3D monoculture of HepG2 cells (3D-Hep) and 2D monoculture of HepG2 cells (2D-Hep), respectively. CAP was added into the iBAC. Live cells stained in green and dead cells stained in red. All data are presented as means ± SD from three independent experiments. $^{**}p < 0.01$, relative to control group.

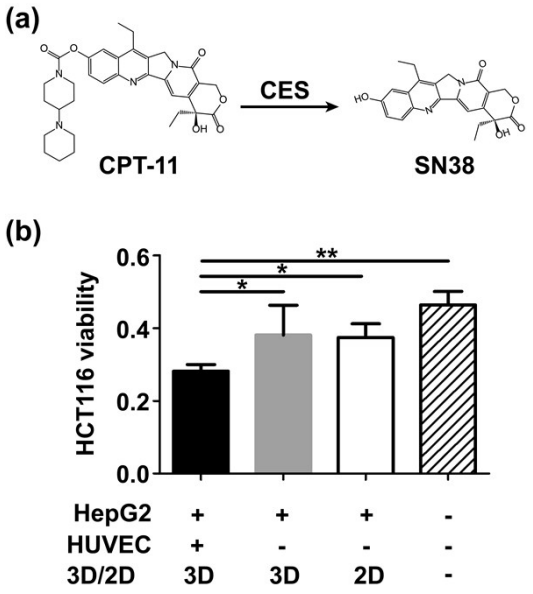

Fig. S6. Metabolic pathway of CPT-11 and comparison of metabolism-induced anticancer bioactivity of the CPT-11 in different co-culture groups on the iBAC. (a) Main metabolic pathway of the CPT-11. (b) Viabilities of 3D HCT116 cells co-cultured with different liver models were compared by CellTiter Blue on a micro-plate reader. The three liver models were 3D biomimetic liver microtissue (3D-Hep-HUVEC), 3D monoculture of HepG2 cells (3D-Hep) and 2D monoculture of HepG2 cells (2D-Hep), respectively. All data are presented as means ± SD from three independent experiments. *$p < 0.05$ and **$p < 0.01$, relative to control group.

Figure S7

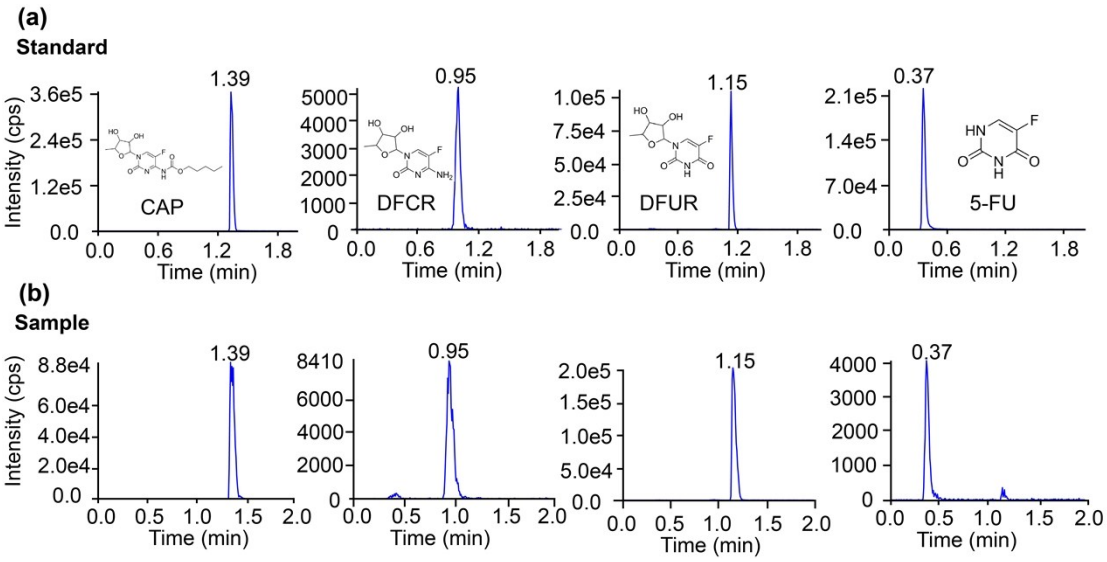

Fig. S7. UPLC-MS characterization of CAP and its metabolites from the iBAC. Comparison of retention times of reference standards (a) with those of samples (b) indicating the metabolites were generated on the iBAC. HepG2-based 3D biomimetic liver microtissue and 3D MCF7 tumor microtissue were co-cultured.

Figure S8

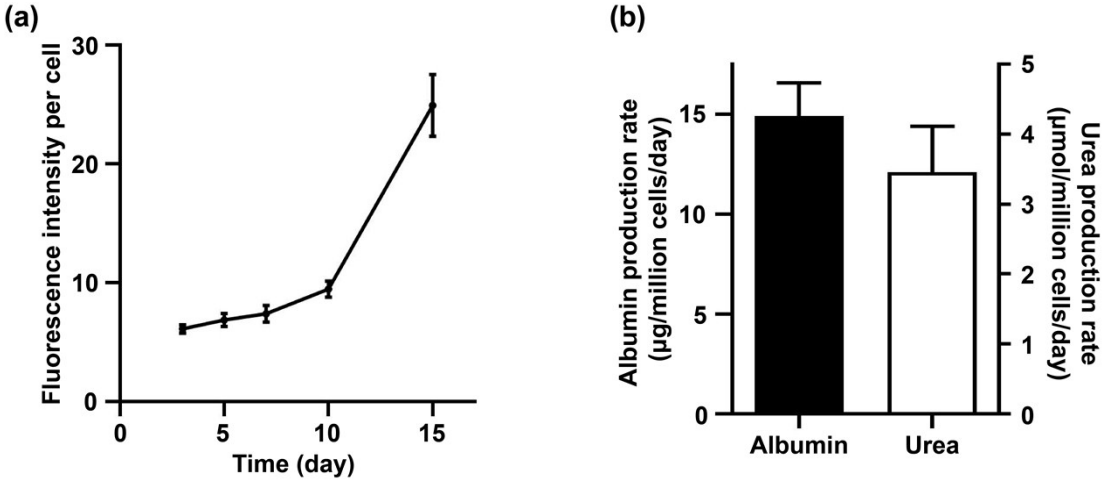

Fig. S8. Evaluation of viability and liver-specific function of primary human hepatocytes (PHHs). (a) Viabilities of PHHs were increased over 15 days. (b) Production of albumin and urea after culturing of PHHs for 15 days. The PHHs were encapsulated in 3D collagen using PHH donor lot GKJ.

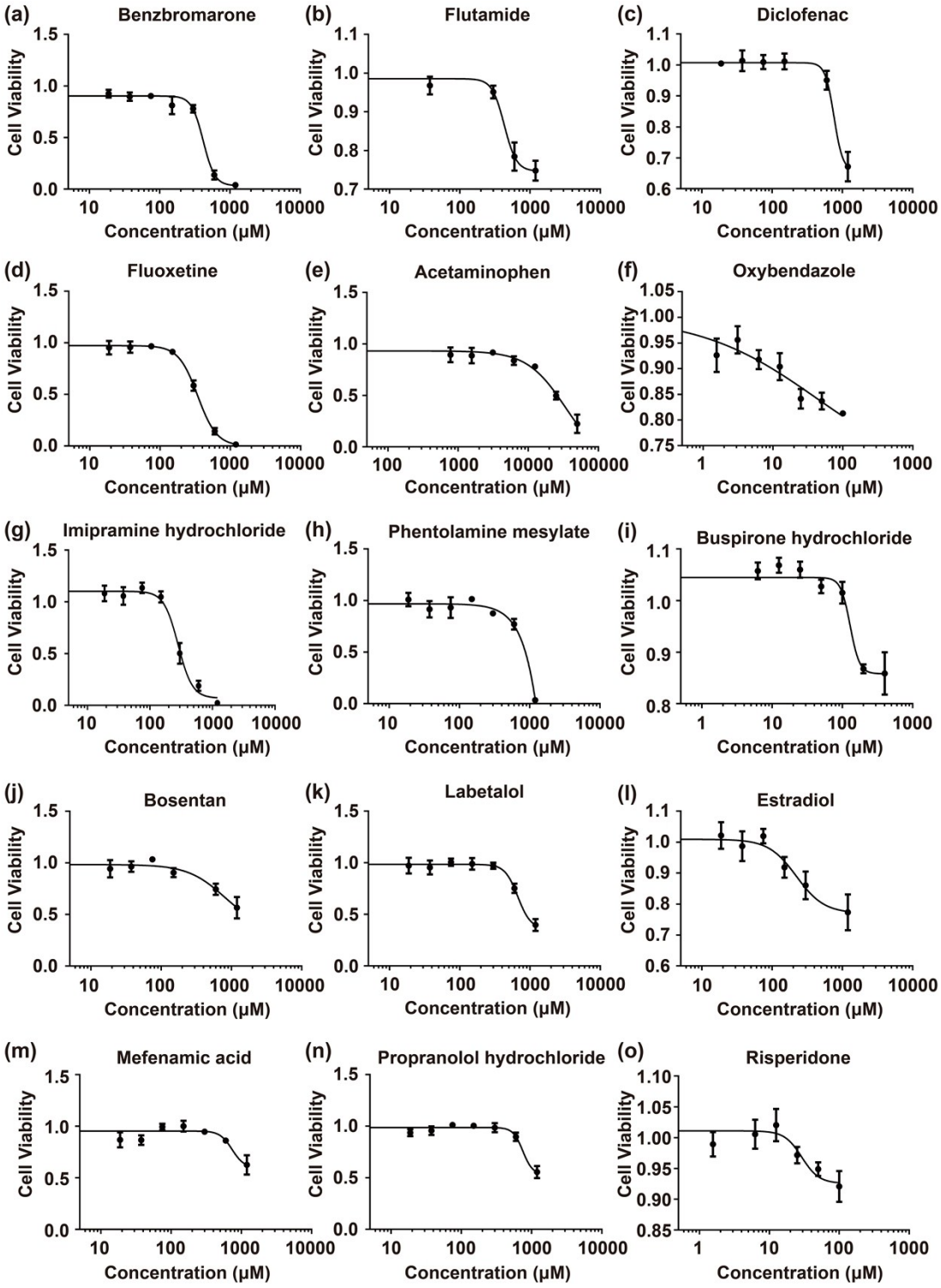

Figure S9. Dose-response curves of 18 model compounds using 3D biomimetic liver microtissues for evaluation of hepatotoxicity.

Table S1 Optimized Q1/Q3 pairs and MS parameters for the detection of CAP and its metabolites.

Compound	Ion mode	Q1(*m*/*z*)	Q3(*m*/*z*)	DP(V)	CE(V)
CAP	Negative	358.2	153.9	-120	-25
5′-DFCR	Negative	244.1	128.1	-80	-20
5′-DFUR	Negative	245.1	129.0	-80	-19
5-FU	Negative	129.0	42.1	-72	-27

Table S2 Donor and clinical information of PHHs used in this study.

Donor	Lot	Sex	Age	Ethnicity	Medications
1	HVN	Male	33	Caucasian	Celexa, Seroquel
2	GKJ	Male	52	Caucasian	Prescription meds for depression/bipolar

Table S3 Comparison of IC_{50} results of drug hepatotoxicity from hepatocytes from different donors.

Drug	IC_{50} from Donor 1 (μM)	IC_{50} from Donor 2 (μM)
Risperidone	100.0	100.0
Oxybendazole	100.0	79.80
Trazodone hydrochloride	220.1	167.1
Mefenamic acid	239.3	316.1

Table S4 Comparison of therapeutic index between iBAC and *in vivo* data.

	iBAC data			*In vivo* data		
Drug	IC_{50} from anticancer bioactivity (μM)	IC_{50} from hepatotoxicity (μM)	Therapeutic index	ED_{50} from anticancer bioactivity	LD_{50} from toxicity	Therapeutic index
Irinotecan	121.3	421.5	**3.5**	32 mg/kg[1]	177.5 mg/kg[1]	**5.5**
Adriamycin	2.146	53.57	**25.0**	1 mg/mg[2]	12.5 mg/kg[3]	**12.5**
Epirubicin	3.647	154.5	**42.4**	4.758 μM[a][4]	108.3 μM[b][5]	**22.8**
Plumbagin	2.956	12.16	**4.1**	3 mg/kg[6]	7.99 mg/kg[6]	**2.7**

Notes: All the *in vivo data* from mice except for [a] from patient-derived gastric cancer organoids and [b] from zebrafish. Therapeutic index is calculated by dividing value of toxicity with value of anticancer bioactivity.

References

1 T. Kunimoto, K. Nitta, T. Tanaka, N. Uehara, H. Baba, M. Takeuchi, T. Yokokura, S. Sawada, T. Miyasaka and M. Mutai, *Cancer Res.*, 1987, **47**, 5944-5947.

2 S. C. Bang, J. H. Lee, G. Y. Song, D. H. Kim, M. Y. Yoon and B. Z. Ahn, *Chem. Pharm. Bull. (Tokyo)*, 2005, **53**, 1451-1454.

3 H. Shindo, T. Ogura, T. Masuno, S. Hayashi and S. Kishimoto, *Cancer Immunol. Immunother.*, 1985, **20**, 145-150.

4 N. G. Steele, J. Chakrabarti, J. Wang, J. Biesiada, L. Holokai, J. Chang, L. M. Nowacki, J. Hawkins, M. Mahe, N. Sundaram, N. Shroyer, M. Medvedovic, M. Helmrath, S. Ahmad and Y. Zavros, *Cell Mol. Gastroenterol. Hepatol.*, 2019, **7**, 161-184.

5 Y. Han, J. P. Zhang, J. Q. Qian and C. Q. Hu, *J. Appl. Toxicol.*, 2015, **35**, 241-252.

6 R. A. Naresh, N. Udupa and P. U. Devi, *J. Pharm. Pharmacol.*, 1996, **48**, 1128-1132.